



## Evaluation of acridine in Nafion as a fluorescence-lifetime-based pH sensor

Title	Evaluation of acridine in Nafion as a fluorescence-lifetime-based pH sensor
Author(s)	Ryder, Alan G.;Power, Sarah;Glynn, Thomas J.
Publication Date	2003

## Evaluation of Acridine in Nafion as a Fluorescence-Lifetime-Based pH sensor.

ALAN G. RYDER,\* SARAH POWER, AND THOMAS J. GLYNN.

*Department of Physics, National University of Ireland-Galway, Galway, Ireland.*

**We report a novel fluorescence lifetime based pH sensing method that utilises acridine incorporated into Nafion (AcNaf) as the fluorescent indicator. The AcNaf sensor is excited using a 380 nm Light Emitting Diode (LED) and the fluorescence lifetimes are measured at 450 and 500 nm. The fluorescence behaviour of acridine as a function of pH in aqueous phosphate buffers and incorporated into the Nafion membrane has been investigated. The results show that incorporating acridine into Nafion changes the apparent ground state  $pK_a$  from ~5.45 to ~9, while the apparent excited state  $pK_a^*$  is only slightly changed (~9.4 in 0.1M phosphate buffer). The AcNaf film shows a good pH response with a change in average lifetime of ~19 ns (at an emission wavelength of 450 nm) over the pH 8 to 10 range. We also show that excited state protonation does not occur in the AcNaf sensor film and that chloride quenching cannot occur because of the permselective nature of Nafion. We also discuss how the unique structure of Nafion affects the fluorescence behaviour of acridine at various pH values, and examine the impact of buffer concentration on apparent  $pK_a$  and pH sensing ability.**

Index Headings: Fluorescence lifetime; acridine; sensor; Nafion; ultraviolet; light emitting diode; pH.

### INTRODUCTION

In the past decade the application of fluorescence lifetime based sensing methods for analytes of clinical significance has become more widespread.<sup>1,2,3</sup> In particular, advances in semiconductor light sources and the miniaturisation of measurement electronics have made time-resolved methods much more practical.<sup>4,5,6</sup> Fluorescence lifetime measurements are less sensitive to photobleaching, source instabilities, and sample turbidity than conventional fluorescence intensity measurements, and can lead to more reproducible results, a critical factor for clinical applications. Analytes such as oxygen,<sup>7</sup> carbon dioxide,<sup>8</sup> halides,<sup>9</sup> and pH,<sup>10</sup> have all been measured with varying degrees of accuracy. Accurate pH sensing is a very important requirement in the clinical, life, and physical sciences. In the case of pH sensing the goal is to achieve high accuracy (better than  $\pm 0.02$  pH units), rapid response, and minimal sample volume. A variety of different fluorophores have been used as sensors for pH measurement including SNARF (semi-naphthorhodafluor) derivatives,<sup>11-12</sup> SNAFL (carboxy-seminaphthofluorescein) derivatives,<sup>1, 13</sup> and LysoSensors.<sup>14</sup> Acridine is another candidate for lifetime based pH sensing because there is a large difference in the fluorescence lifetime of the neutral (6.6 ns) and protonated forms (31.1 ns.) of acridine.<sup>15-16</sup> The ground state  $pK_a$  in aqueous solution is 5.45, which makes it useful

for pH sensing of biological systems. Unfortunately, there are two significant drawbacks with employing acridine as a pH sensor: 1) It undergoes excited state protonation because it has an excited state  $pK_a^*$  of 10.7, and 2) Acridine is dynamically quenched by halide ions.<sup>17</sup>

A key factor in developing a fluorescence sensor is the choice of matrix in which the sensing fluorophore can be supported. For pH sensing, the support must allow the free passage of hydrogen ions, prevent leaching of the fluorophore, and be flexible enough for incorporation into functional devices. Nafion, a commercial perfluorinated ionomer film, which is a copolymer of tetrafluoroethylene (Teflon) and perfluoro-3,6-dioxo-4-methyl-7-octene-sulfonic acid has excellent ion transport and ion exchange properties, and furthermore it is permselective passing only cations and not anions.<sup>18</sup> This is a result of its unique structure, which consists of a fluorocarbon backbone with pendant chains terminated with sulfonate head groups (Fig. 1). The hydrophobic fluorocarbon backbone ensures the polymer has excellent chemical, thermal, and mechanical stability. The strongly hydrophilic sulfonate groups, which have a very high water of hydration (~thirteen molecules of water for every sulfonate group) produce the excellent cation transport ability of the polymer. These sulfonate groups also confer ion exchange properties on the polymer, as  $H^+$  ions can be exchanged with a larger cation such as sodium by stirring the film in NaOH solution.<sup>19-20</sup>

The microstructure of Nafion has been investigated spectroscopically using fluorescence and absorption methods.<sup>21-22</sup> It has been proposed that the microstructure may be understood in terms of a reverse micelle-like ion cluster model. According to this model, there are three distinctive regions within the polymer: ion clusters, which consist of a hydrophilic water core, surrounded by an interfacial region, and supported by the hydrophobic fluorocarbon backbone. This model presumes that the water cores in neighbouring ion clusters are interconnected through channels, thus facilitating ion transport through the membrane. An alternative three region structural model was proposed based on diffusion studies within Nafion. In this model the ion clusters are assumed to be amorphous, formed by the fluorocarbon backbone surrounding a region with high water and ionic sulfonate groups. The interfacial region consists of a mixture of pendant side chains, small amounts of water, non-clustered sulfonate exchange sites, and counter ions.

Received 26 March 2002; accepted 2 September 2002.

\* Author to whom correspondence should be sent.

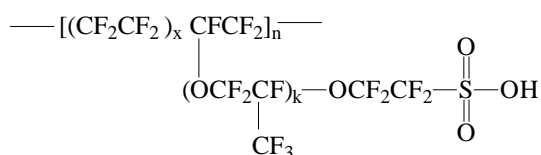


**FIG 1:** Chemical structure of Nafion (acid form).

Fluorescence spectroscopic probing has yielded further information on the interfacial region of Nafion and it suggests that dyes tended to locate in this zone. It also appears that the interfacial region represents a substantial if not the dominant morphology of the polymer,<sup>19</sup> and that these regions can accommodate considerable molecular diffusion. This interfacial region, while consisting primarily of perfluorinated polymer branches and water molecules, is actually inhomogeneous consisting of two distinct zones of different polarity similar to that of polar organic solvents. It has been proposed that the zone closest to the polymer backbone is more hydrophobic due to a higher content of polymer branches, while the zone close to the water core is probably more hydrophilic due to more water molecules in the heterogeneous mixture. These structural models are largely based on fluorescence lifetime studies of ethidium bromide in Nafion, which show that the fluorescence decay is a bi-exponential process indicating that the fluorophore can reside in two sites of different polarities within Nafion.<sup>22</sup>

In this study, we examine acridine incorporated into Nafion (AcNaf) as a potential pH sensor. We describe how its unique anionic permselective structure prevents chloride quenching and influences the fluorescence behaviour of acridine by shifting its  $pK_a$  to higher pH thus preventing excited state protonation.

## EXPERIMENTAL

**Instrumentation.** Fluorescence steady state spectra were recorded using a Perkin-Elmer LS-50B luminescence spectrometer and absorption spectra were measured using a Shimadzu UV-1601 spectrometer. Fluorescence lifetimes were measured using an in-house assembled lifetime measurement system that has been described previously.<sup>16,23</sup> The system uses the Time Correlated Single Photon Counting (TCSPC) measurement method, interchangeable Light Emitting Diode (LED) and laser diode excitation sources, and interference filters for selecting the desired emission wavelength. In this study, we used a pulsed 380 nm LED (PLS370, PicoQuant GmbH, Germany) as the excitation source and measured the Instrument Response Function (IRF) using a non-fluorescent suspension of alumina in water. All measurements were made in 1 or 10 mm pathlength quartz cells from either front surface excitation or 90-degree geometries as appropriate. Fluorescence lifetimes were extracted from the measured decay curves using the FLUOFIT program ver. 3.0 (PicoQuant) with the final quoted results being determined by the fit which had a  $\chi^2$  (goodness of fit) value of less than 1.2 and a residual trace that was symmetric about the zero axis. Average lifetime ( $\bar{\tau}$ ) were calculated using equation (1),<sup>24</sup> which is implemented by the FLUOFIT software:

$$\text{Average Lifetime } (\bar{\tau}) = \frac{\sum_0^I \alpha_i \tau_i^2}{\sum_0^I \alpha_i \tau_i} \quad \text{Eqn. (1)}$$

where  $\alpha_i$  is the pre-exponential factor, reflecting the relative contribution of a fluorescent species with a lifetime  $\tau_i$ .

The accuracy of individual fluorescence lifetimes was given by the confidence interval calculated by the support plane method implemented by the software.<sup>25-26</sup> For the error in average lifetimes, we used a modification of the method where  $\bar{\tau}$  was plotted against  $\chi^2$  for a series of fits in which a single lifetime component was systematically varied while the remaining components were held fixed. The method is tedious but, we have found in practice that the average lifetimes are accurate to better than  $\pm 0.1$  ns.<sup>27</sup> Sigmoidal fits and plots were generated using EasyPlot 4.0 (Spiral software & MIT).

**Materials.** Acridine and buffer chemicals were purchased from Sigma-Aldrich and used without any further purification. All buffers were made up in deionised water and most solutions were not degassed or de-aerated before use unless otherwise stated. Nafion<sup>®</sup> 117 membrane (hydrogen ion form) was purchased from Sigma-Aldrich and could be purified by stirring the film in concentrated nitric acid at 60°C for twenty-four hours. Both purified and unpurified films were used in order to investigate the necessity of such a purification procedure. The sodium form of Nafion was generated by stirring the film in 1M NaOH for 24 hours.

**Data analysis:** Ground state  $pK_a$  values for acridine in solution and Nafion film were obtained from the absorption spectra recorded over a range of pH values. The spectra were first baseline corrected and then normalised to their integral area to minimise out any concentration effects caused by possible leaching of dye from the film, or cuvette positioning effects.<sup>†</sup> The relative absorbance at 380 nm was then measured and plotted as a function of pH, yielding a sigmoidal curve. The  $pK_a$  value is taken as the pH value at the point of inflection of the sigmoidal curve, which was normally obtained by taking the first derivative plot of the sigmoidal curve. The  $pK_a$  was also calculated using the Henderson-Hasselbach equation, which yielded similar values. In the case of immobilised indicators, there is not a single (thermodynamic)  $pK_a$ , but rather an apparent  $pK_a$ , because of the dye being located in a heterogeneous microenvironment.<sup>28-29</sup>

Excited state  $pK_a^*$  values were calculated from plots of fluorescence emission intensity ratios and average lifetime versus pH using the method outlined above. Fluorescence emission intensity ratios were used instead of single wavelength intensity values to negate any measurement variations introduced by light source or detector instability, photobleaching, cuvette positioning, or leaching of the dye from the film.<sup>30</sup> We have used the fluorescence intensity ratios at 450/500 nm and at 500/450 nm in the Henderson-Hasselbach equation for calculating  $pK_a^*$ , in order to eliminate any variation due to measurement errors. The  $pK_a^*$  values were also calculated using the Förster cycle

<sup>†</sup> The spectra cannot be normalised to their maximum peak, as this is pH sensitive.

method but this yields higher values than the other methods outlined above.

## RESULTS AND DISCUSSION

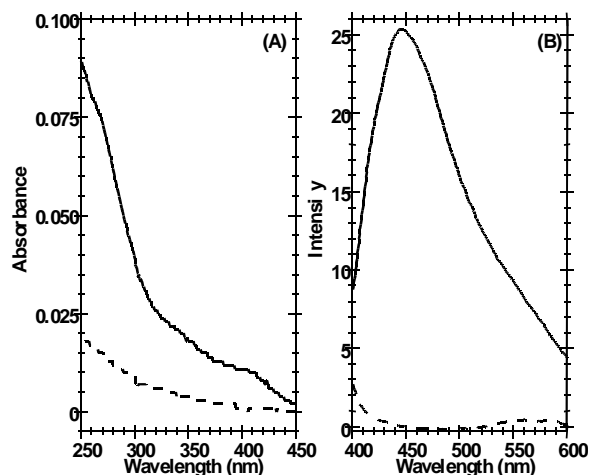


**FIG. 2:** Absorption (A) and fluorescence emission spectra (B) of unpurified (—) and purified (---) Nafion. Excitation wavelength 380 nm.

Nafion film as supplied has a slight brownish tint and it has been reported that excitation in the UV region gives an emission band at 390 nm.<sup>22</sup> This colouration can be removed by acid treatment at elevated temperatures,<sup>20</sup> which results in a weaker absorption spectrum (Fig. 2A). The fluorescence emission spectra (Fig. 2B) of both Nafion films excited at 380 nm show that the weak emission band at 450 nm present in the unpurified film is completely removed by the acid treatment. We have found in practice that there was very little difference between using either form of Nafion because these impurity levels are very low. For example, we were not able to obtain an accurate fluorescence lifetime measurement of this very weak emission band at 450 nm even with prolonged measurement times. When acridine is incorporated into Nafion there is scarcely any difference in the absorption spectra as shown in Fig. 3 because the absorption of acridine is so much stronger than that of the impurities. Furthermore, neither the fluorescence emission spectra nor the fluorescence lifetimes (Table 1) of the acridine loaded films showed any significant differences between the use of purified or unpurified Nafion film.<sup>27</sup>

Emission wavelength (→)	450 nm	500 nm		
Sample (↓)	$\tau$ (ns)	$\chi^2$	$\tau$ (ns)	$\chi^2$
Acid solution (AcH <sup>+</sup> *)	31.56 ± 0.15	1.10	31.55 ± 0.13	1.06
Base solution (Ac*)	6.55 ± 0.035	1.04	6.59 ± 0.03	1.19
Purified AcNaf in acid	33.18 ± 0.13	1.09	33.09 ± 0.13	1.20
Unpurified AcNaf in acid	32.98 ± 0.16	1.20	32.93 ± 0.16	1.20
Purified AcNaf in base	6.86 <sup>‡</sup>	1.05	9.97 <sup>‡</sup>	1.03
Unpurified AcNaf in base	6.79 <sup>‡</sup>	1.04	9.88 <sup>‡</sup>	1.06

<sup>‡</sup> Average fluorescence lifetimes.

**Table 1:** Fluorescence lifetimes of acridine in solution, and in Nafion film (AcNaf), in aqueous 1M HNO<sub>3</sub> acid and 1M NaOH. Excitation wavelength 380 nm. Errors calculated by support plane analysis.

Acridine is readily absorbed into Nafion film from ethanolic or aqueous solutions, with very little leaching observed over the pH ranges employed in this study.<sup>27</sup> There is very little difference in the absorption spectra of acridine in Nafion (AcNaf) and acridine in solution, under acid (Fig. 3A) or base (Fig. 3B) conditions, with both having absorption maxima at 354.5 nm. The most substantial difference between the neutral acridine (Ac) and protonated acridinium cation (AcH<sup>+</sup>) is a broad band extending out to ~445 nm due to the AcH<sup>+</sup> species for both solution and AcNaf. Although the profile of the absorption spectra is unchanged in Nafion, the absorption in solution is slightly stronger and so it appears that loading acridine into Nafion does not greatly affect the ground state of either the neutral or protonated forms of acridine

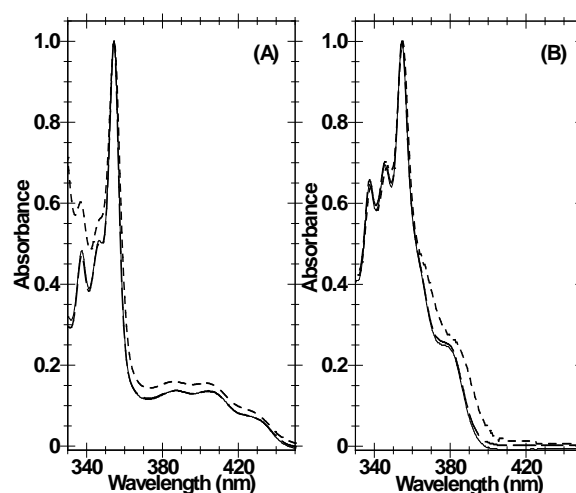


**FIG. 3:** Absorption spectra of  $0.5 \times 10^{-4}$  M acridine in solution (---), and loaded into purified (—) and unpurified (---) Nafion recorded in A). 1M HNO<sub>3</sub> showing the protonated AcH<sup>+</sup> absorption, and B). 1M NaOH showing the neutral Ac absorption. Spectra were normalised at absorption wavelength 354.5 nm.

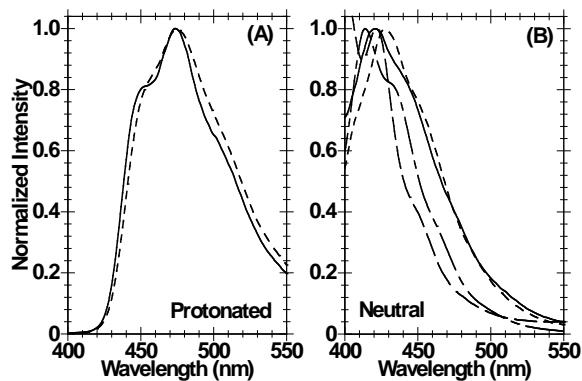


**FIG. 4:** A). Normalised fluorescence emission spectra recorded in 1M HNO<sub>3</sub> of acridine in solution (---), and loaded into Nafion (—). B). Normalised fluorescence emission spectra of acridine in 1M NaOH (---), acridine in Nafion in 1M NaOH (—), acetone (---) and ethanol (---). Excitation wavelength 380 nm, bandpass 10 nm.

The weak absorbance of the neutral and protonated acridine species over the 370 to 390 nm range is still sufficient for reasonable excitation efficiency using a 380 nm LED. The steady state fluorescence emission spectra taken using 380 nm excitation shows that the AcH<sup>+</sup>\* in solution (asterisk denotes excited state) has a fluorescence maximum at 475 nm (Fig. 4A) and that there is a small hypsochromic shift to 473 nm for AcNaf in acid. Another difference between solution and AcNaf in acidic conditions is the pronounced shoulder present at 450 nm in the AcNaf spectrum which is less evident in AcH<sup>+</sup>\* solution emission. The neutral Ac\* species in solution fluoresces at a shorter wavelength ( $\lambda_{max} = 430$  nm) which are in good agreement with values reported elsewhere (Fig. 4B).<sup>15,31</sup> The most significant difference on loading acridine into Nafion occurs with the emission spectrum, which while having the same profile, is blue shifted by 10 nm with respect to Ac\* in solution. The general similarity between the film bound acridine and the solution spectra would indicate that AcNaf should have significant pH sensing ability.

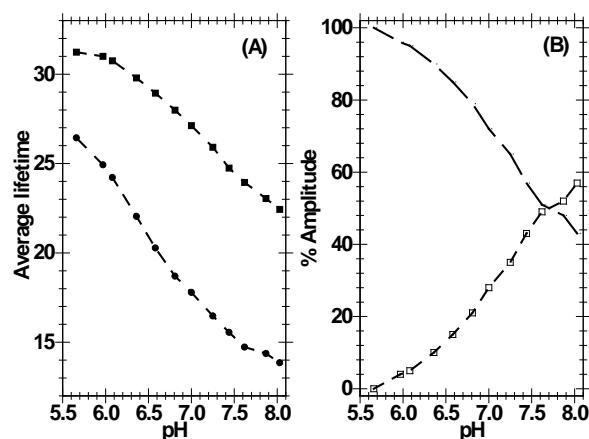


**Fig. 5:** A). Average lifetime of acridine in 0.1M phosphate buffer, plotted as a function of pH at two emission wavelengths, 450 nm (●) and 500 nm (■). B). % amplitude of  $\tau_1$  (○) and  $\tau_2$  (□) plotted as a function of pH. Data obtained from fluorescence lifetimes measured at 500 nm for Acridine in 0.1M phosphate buffer.

#### Fluorescence lifetime behaviour of acridine in Nafion.

There is a very large difference in the mono-exponential fluorescence lifetimes of Ac and AcH<sup>+</sup>\* in aqueous solution measured at emission wavelengths of 450 nm and 500 nm using the 380 nm LED excitation (table 1). The protonated AcH<sup>+</sup>\* species in solution has a relatively long lifetime of approximately 31 ns while the lifetime of neutral Ac\* in 1M NaOH is considerably shorter at around 6.6 ns and these results are similar to those reported elsewhere.<sup>15</sup> Plotting the variation in the average fluorescence lifetime (Fig 5A) of acridine in 0.1M phosphate buffer over the pH range 5.7-8.0 shows a significant effect over this biologically significant range. At wavelength of 450 nm, emission occurs from both the AcH<sup>+</sup>\* and Ac\* species yielding a bi-exponential decay. The decay time for each species remains relatively constant, but the fractional amount of each species varies considerably with pH (Fig. 5B). As the pH increases, neutral acridine begins to appear, resulting in a bi-exponential decay and a drop in the average lifetime. At an emission wavelength of 500 nm, the decay curve obtained at pH 5.7 fits to a single exponential lifetime of 31 ns, indicating that AcH<sup>+</sup>\* is the sole emitting species at this pH. At any given pH, the average lifetime measured at an emission wavelength of 500 nm is longer than that measured at 450 nm because of the greater contribution of the protonated species.

At pH values greater than 12, the average fluorescence lifetime of AcNaf in phosphate buffer begins to decrease again and at these pH values there is no variation in the relative absorption as a function of pH, indicating there is no effect on the ground state properties of acridine in Nafion.<sup>27</sup> At these high pH levels, it is probable that the remaining AcH<sup>+</sup>\* is being deprotonated, resulting in a decrease in the measured fluorescence lifetime. The effect is more noticeable at longer wavelengths because of the greater emission intensity of AcH<sup>+</sup>\* at longer emission wavelengths.

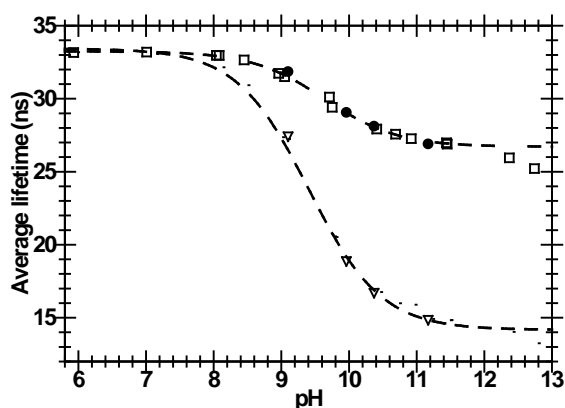


**Fig. 6:** Plot of average fluorescence lifetime of acridine in Nafion versus pH at two emission wavelengths: 450 nm (o) unpurified Nafion, purified (V) Nafion and 500 nm (□) unpurified Nafion, (●) purified Nafion. Measurements taken with front surface excitation using a 380 nm LED in 0.1M phosphate buffer.

When acridine is incorporated into Nafion this large difference in lifetime between protonated and neutral species is maintained at both emission wavelengths (Table 1). In the case of AcNaf in 1M acid, the decay is mono-exponential with long lifetime of  $\sim 33$  ns. This is slightly longer than that obtained in solution and is probably due to a degree of stabilisation offered by the anionic nature of the polymer.

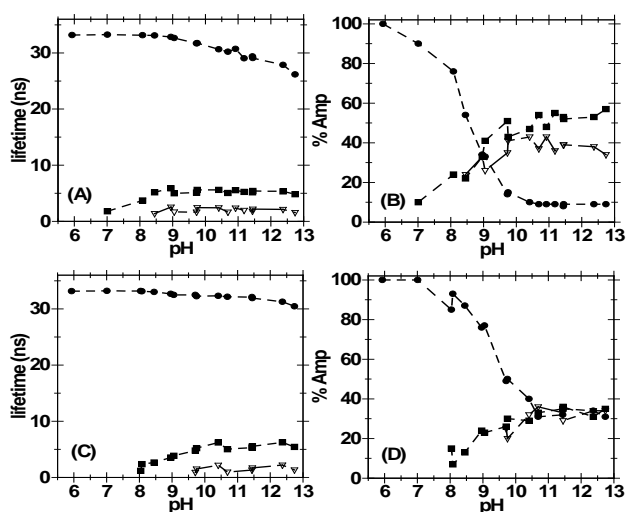


**Fig. 7:** Influence of pH on the fluorescence decay of acridine in Nafion at different pH (0.1M phosphate buffer). 1, 2, and 3 decay time models were employed (lifetimes  $\tau_1$  (●),  $\tau_2$  (■),  $\tau_3$  (V) and amplitudes (in %)  $\alpha_1$  (●),  $\alpha_2$  (■), and  $\alpha_3$  (V)). A) Plot of lifetimes versus pH for 450 nm emission; B) Plot of amplitudes versus pH for 450 nm emission; C) Plot of lifetimes versus pH for 500 nm emission; D) Plot of amplitudes versus pH for 500 nm emission;

In contrast, the situation for AcNaf under strongly basic conditions is more complex with a triple exponential model being required to fit the decay curve adequately. The calculated average lifetime is between 6.8 and 10 nanoseconds, depending on the emission wavelength, and consists of three species: a long lifetime component ( $\tau_1$ ) of 10-14 ns, a  $\sim 4$ -5 ns component ( $\tau_2$ ), and a fast decay component ( $\tau_3$ ) of under 1 ns. These three different components are a result of the heterogeneous nature of the Nafion polymer.

It is likely that neutral acridine ( $Ac^*$ ) is located in the heterogeneous interfacial region within Nafion and not in the hydrophobic backbone region because it is still sensitive to changes in the pH of an aqueous solution. In this heterogeneous interfacial region, acridine can exist in both protonated and neutral forms and in particular, the neutral species is subject to different environments with varying polarity. There is a similar pattern of behaviour in the fluorescence decays observed for ethidium bromide in Nafion and in solution.<sup>19-20</sup> It seems likely that the long lifetime component derives from traces of  $AcH^{+*}$  residing in the highly polar aqueous zones within the polymer. In these zones, the acridine molecules would be in close contact with the anionic sulphonate groups and one would expect that a small amount of the acridine would remain in the protonated form even at very high pH ( $>12$ ). This is further supported by the fact that the lifetime increases on going from 450 to 500 nm, where the emission of  $AcH^{+*}$  is much stronger than  $Ac$ . The second lifetime component  $\tau_2$ , is due to emission from  $Ac^*$  residing in the less charged, interfacial region, in an environment with a polarity comparable to water. Finally, we would propose that the fast lifetime component  $\tau_3$ , is a result of emission from  $Ac^*$  residing in the more hydrophobic area of this interfacial region close to the perfluorinated backbone of the polymer. Evidence to support this comes from the fluorescence lifetime of  $Ac^*$  in methanol (377 ps), ethanol (370 ps), and hexane (45 ps), where it is clear that, as solvent polarity decreases, the fluorescence lifetime of  $Ac^*$  decreases.<sup>32</sup> Furthermore, the steady state emission spectra (Fig. 4B) of acridine in acetone shows that the  $Ac^*$  emission maximum is blue shifted (to  $\sim 421$  nm) with respect to aqueous solution, but at a similar wavelength to that of AcNaf. In ethanol, emission is blue shifted further to  $\sim 414$  nm, even further than  $Ac^*$  in both aqueous solution and Nafion.

The measured average fluorescence lifetime of AcNaf varies considerably with pH (Fig. 6), with a change of  $\sim 17$  ns at 450 nm and  $\sim 6$  ns at 500 nm, over the range pH 8 to 11. At both emission wavelengths, the fluorescence decay of AcNaf is a single exponential below pH 7.0, due to emission solely from  $AcH^{+*}$  (Fig. 7). Above pH 7 the fit becomes bi-exponential, indicating the presence of a second emitting species  $Ac^*$ , with a short lifetime of  $\sim 5$  ns. As the pH increases further, a third lifetime component, with a fast decay time of less than 2.5 ns, appears. The decay times for each lifetime component remain relatively constant (Fig. 7A & C), but the fractional contribution of each component to the overall decay varies as a function of pH (Fig. 7B & D). As the pH increases the percentage of the fluorophore in the excited protonated state decreases, so there is less of a contribution from the long lived  $AcH^{+*}$  species.

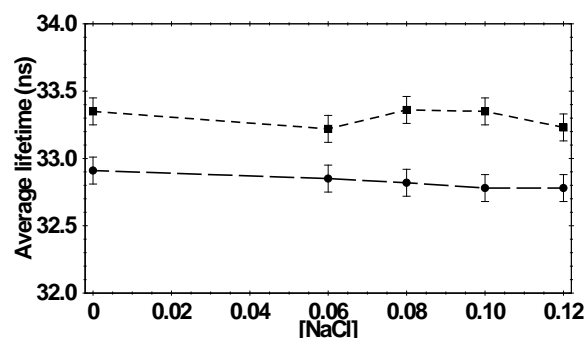


**Fig. 8:** Average lifetime plotted as a function of NaCl concentration at emission wavelength 450 nm (●) and 500 nm (■) for acridine loaded Nafion in 0.1M phosphate buffer at pH 7.4.

**Effect of chloride ion concentration:** The presence of chloride ions has a negligible effect on the average fluorescence lifetime of AcNaf as shown in Fig. 8.<sup>‡</sup> When compared to the quenching of acridine in solution (Fig. 9A & 9B) the difference is very dramatic and indicates that no quenching is occurring. The dynamic quenching of acridine fluorescence by halides occurs primarily with the AcH<sup>+</sup>\* species. Fig. 9C shows Stern-Volmer plots for steady state emission spectral data at two different pH values, pH 5.6 and 7.4, and this non-linear behaviour indicates that the two fluorescence species Ac and AcH<sup>+</sup>\* are unequally quenched by chloride. <sup>33-34</sup> In this case, a modified version of the Stern-Volmer equation (Equation 2) is used to account for the unequal quenching rates. This is based on the assumption that the intensity of the accessible fraction of the fluorescence will be Stern-Volmer quenched, while the inaccessible fraction will be unaffected.

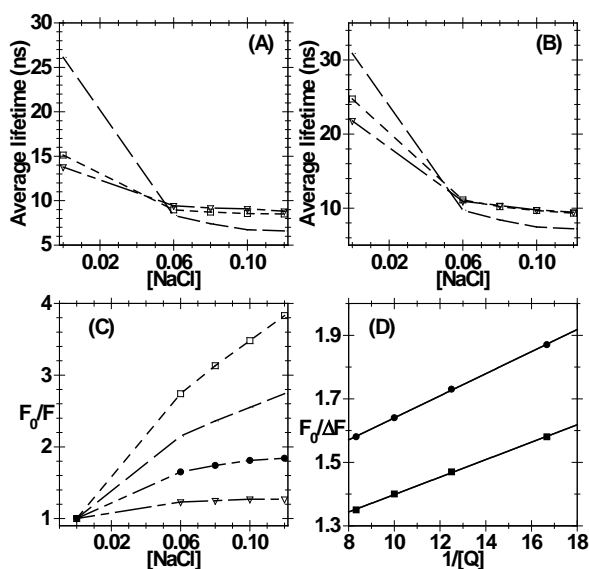


**Fig. 9:** (A) Plot of average lifetime measured at 450 nm versus NaCl concentration for acridine in 0.1M phosphate buffer at: pH 5.6 (o), pH 7.3 (□), pH 7.9 (∇); (B) Plot of average lifetime measured at 500 nm versus NaCl concentration for acridine in 0.1M phosphate buffer at: pH 5.6 (o), pH 7.3 (□), pH 7.9 (∇); (C) Stern-Volmer plots for quenching of acridine by chloride. Based on steady state fluorescence intensity at two wavelengths: 450 nm: pH 5.6 (o), and pH 7.3 (∇); and 500 nm: pH 5.6 (□), and pH 7.3 (●). (D) Modified Stern-Volmer plots for quenching of acridine by chloride at pH 5.6, from steady state fluorescence intensity at 450 nm (●) and 500 nm (■).

The equation takes the form:

$$\frac{F_0}{\Delta F} = \frac{1}{f_a K_{sva} [Q]} + \frac{1}{f_a} \quad \text{and} \quad f_a = \frac{F_{0a}}{F_{0a} + F_{0b}} \quad \text{Eqn. 2}$$

where  $\Delta F = F_0 - F$ , and  $K_{sva}$  is the Stern-Volmer quenching constant of the accessible fraction.  $F_{0a}$  and  $F_{0b}$  are the intensities of the accessible and inaccessible fractions of the fluorophore in the absence of quencher and therefore  $f_a$  is the fraction of the initial fluorescence that is accessible to the quencher. If the quenching data fits the model, then a plot of  $F_0/\Delta F$  against  $1/[Q]$  should be linear with  $1/(f_a K_{sva})$  as the slope, and  $1/f_a$  as the intercept. The modified Stern-Volmer plots (Fig. 9D) for acridine quenching by chloride are linear thus indicating that the protonated AcH<sup>+</sup>\* species is dynamically quenched by chloride while the neutral Ac\* is unaffected. In further work we also established that a number of common buffers such as MOPS, HEPES, and BIS-TRIS also caused quenching of acridine fluorescence in solution, thus further limiting its usefulness as a pH indicator.<sup>27</sup>

In the case of AcNaf, the halide sensitive, charged AcH<sup>+</sup>\* species is located deep within the Nafion membrane, and is therefore very inaccessible to chloride ions. This anion exclusion enables AcNaf to be used as a pH sensor in environments with very high halide (or other anionic quenchers) concentrations.

Conc. of buffer	0.05M	0.10M	0.20M
Apparent pK <sub>a</sub> (from absorbance at 380 nm)	9.48	9.09	8.68
Apparent pK <sub>a</sub> * (at λ = 450 nm)	9.80	9.39	9.20
Apparent pK <sub>a</sub> * (at λ = 500 nm)	9.99	9.65	9.44
ΔpK <sub>a</sub> (450 nm)	0.32	0.30	0.52
ΔpK <sub>a</sub> (500 nm)	0.51	0.56	0.76

**Table II:** pK<sub>a</sub> data for acridine loaded Nafion in phosphate buffers. ΔpK<sub>a</sub> is the difference between the apparent pK<sub>a</sub> (ground state) and apparent pK<sub>a</sub>\* (excited state).

**Excited state protonation effect:** Acridine in solution has a reported ground state pK<sub>a</sub> of 5.45, but has an excited state pK<sub>a</sub>\* of 10.6, and therefore tends to gain a proton on promotion to the excited state.<sup>34</sup> AcNaf, however, does not fulfil the criteria for excited state protonation, namely that there must be a large difference between ground pK<sub>a</sub> and excited state pK<sub>a</sub>\* values. This difference (ΔpK<sub>a</sub>) for acridine in Nafion in phosphate buffer was calculated using the apparent pK<sub>a</sub> and pK<sub>a</sub>\* values calculated from first derivatives of the pH titration curves. The apparent ΔpK<sub>a</sub> is less than 0.52 pH units at 450 nm and 0.76 pH units at 500 nm (Table 2).

<sup>‡</sup> The concentration of added NaCl was chosen to mimic the chloride levels of normal blood serum that is approximately 100 mmol/L.

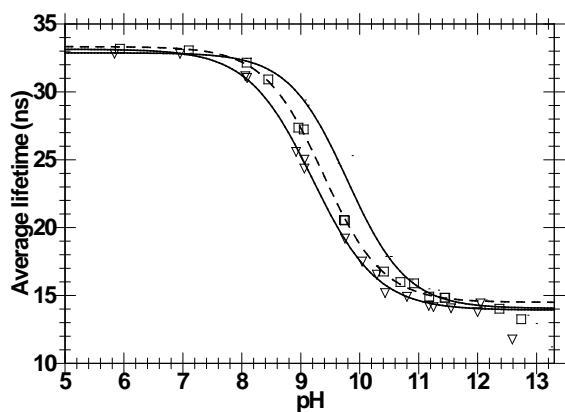


**Fig. 10:** Plot of average fluorescence lifetime (measured at 450 nm) versus pH for acridine loaded Nafion in phosphate buffer of varying molarity: 0.05M (o), 0.10M (□), and 0.20M (Δ).

For excited state reactions, the  $\Delta pK_a$  would normally have a value greater than 4 pH units, and so this indicates that the AcNaf system does not undergo an excited state protonation reaction. Another characteristic of an excited state protonation reaction is the invariance of the absorption spectrum under conditions where the fluorescence emission (intensity or lifetime) spectrum shows pH variance.<sup>34</sup> In the case of AcNaf, the change in average lifetime versus pH occurs over a similar pH range to that of absorption versus pH, which implies that acridine in Nafion, does not undergo an excited state protonation reaction. Another factor that indicates that there is no excited state protonation is the fact that both excited and ground state apparent  $pK_a$  values are equally affected by variations in the buffer concentration. And finally, the fluorescence lifetime decreases as buffer concentration increases (Figs. 10 and 11); this is the opposite to what would be expected with excited state protonation reaction, where the lifetime would have to increase as buffer concentration increases.

**Effect of buffer concentration.** The average lifetime of acridine in solution increases with increasing phosphate buffer concentration because acridine undergoes an excited state protonation reaction.<sup>34</sup> In the case of AcNaf, there is also a change in the average fluorescence lifetime due to changing buffer concentration (Figs. 10 and 11). This is not due to excited state protonation but rather due to ionic strength effects. It has been reported that the  $pK_a$  and  $pK_a^*$  values of immobilised indicators decreases with increasing ionic strength of the buffer.

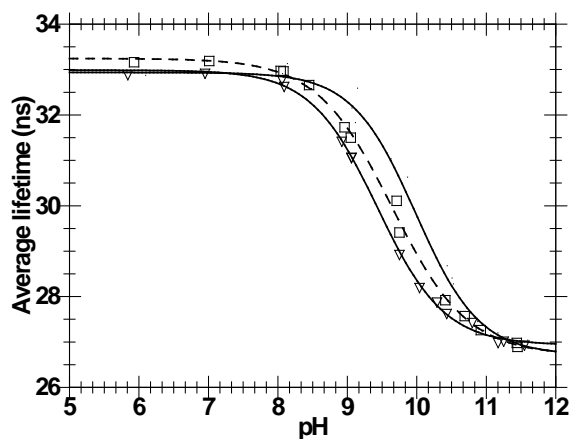


**Fig. 11:** Plot of average fluorescence lifetime (measured at 500 nm) versus pH for acridine loaded Nafion in phosphate buffer of varying molarity: 0.05M (o), 0.10M (□), and 0.20M (Δ).

This effect is due to the change in ionic strength shifting the dissociation equilibrium of the indicator.<sup>29,35-36</sup> This same effect is seen in AcNaf (Figs. 10 and 11), indicating that the dissociation equilibrium of acridine is being affected by variations in ionic strength. The fluorescence lifetime fitting data supports this conclusion, as we have observed that the percentage amplitudes of the lifetime components of AcNaf vary with buffer concentration, while the lifetime values remained constant at the values shown in Figs. 6A and 6C. This effect of ionic strength unfortunately cannot be distinguished from signal changes caused by pH and therefore introduces pH errors. Although the effects of ionic strength cannot be eliminated, they can reportedly be minimised by employing an indicator with a small charge, by chemical modification of the sensor surface, or by calibrating the sensor with an appropriate buffer whose ionic strength is close to that of the sample to be analysed.<sup>37</sup> For AcNaf it is likely that calibration of the average lifetime with an appropriate buffer will enable the use of AcNaf as a working pH sensor.

## CONCLUSION

The ground and excited state  $pK_a$  of acridine are shifted to higher pH on incorporation into a Nafion membrane. The apparent  $pK_a$  values of acridine in Nafion (AcNaf) are found between pH 8.6 and 10, for both ground and excited states, depending on emission wavelength and buffer concentration. Acridine therefore does not undergo excited state protonation reactions when loaded into Nafion because there is no longer a large difference between  $pK_a$  and  $pK_a^*$ . Additionally, the anion exclusion properties of Nafion prevents fluorescence quenching due to halide ions while still permitting the free transport of protons thus enabling pH sensing. However, this also means that the sensing range has shifted from pH 6 – 8 of acridine in solution to pH 8 – 11 for the AcNaf sensor.

The average fluorescence lifetime of AcNaf is, however, affected by changes in ionic strength. This is a result of changes in acridine dissociation which modifies the  $pK_a$  and  $pK_a^*$  values, shifting the pH response curves. It is still feasible to use acridine in Nafion as a pH sensor for solutions or environments of known ionic strength, where the sensor can first be calibrated in buffers of similar ionic strength. We are continuing to develop the AcNaf sensor and are investigating methods that will correct for the variation in fluorescence lifetime with ionic strength.

## ACKNOWLEDGEMENTS

This work was assisted by a Millennium Research Grant from the National University of Ireland-Galway, an Enterprise Ireland Research Innovation Fund award (IF/2001/061), and by the National Centre for Biomedical Engineering Science as part of the Irish Higher Education Authority Programme for Research in Third Level Institutions.

## REFERENCES

- 1 J. R. Lakowicz and H. Szmazinski, *Sens. Actuators B.* **11**, 133 (1993).
- 2 H. Szmazinski and J. R. Lakowicz, "Lifetime-Based Sensing", in Topics in fluorescence spectroscopy: vol. 4. Probe design and chemical sensing, J. R. Lakowicz, Ed., (Plenum Press, New York, 1994), p. 295.
- 3 O. S. Wolfbeis, I. Klimant, T. Werner, C. Huber, et al. *Sens. Actuators B.* **51**, 17 (1998).
- 4 T. Araki and H. Misawa, *Rev. Sci. Instrum.* **66**, 5469 (1995).
- 5 H. Szmazinski and Q. Chang, *Appl. Spectrosc.* **54**, 106 (2000).
- 6 J. Sipiior, G. M. Carter, J. R. Lakowicz, and G. Rao, *Rev. Sci. Instrum.* **68**, 2666 (1997).
- 7 G. A. Holst, T. Köster, E. Voges and D. W. Lübbers, *Sens. Actuators B.* **29**, 231 (1995).
- 8 J. Sipiior, S. Bambot, M. Romauld, G. M. Carter, J. R. Lakowicz, and G. Rao, *Anal. Biochem.* **227**, 309 (1995).
- 9 H. Szmazinski and J. R. Lakowicz, *Sens. Actuators B.* **60**, 8 (1999).
- 10 S. Draxler, M.E. Lippitsch, and M. J. P. Leiner, *Sens. Actuators B.* **11**, 421 (1993).
- 11 A. Srivastava and G. Krishnamoorthy, *Anal. Biochem.* **249**, 140 (1997).
- 12 H. Szmazinski and J. R. Lakowicz, *Anal. Chem.* **65**, 1668 (1993).
- 13 R. Sanders, A. Draaijer, H. C. Gerritsen, P. M. Hout, and Y. K. Levine, *Anal. Biochem.* **227**, 302 (1995).
- 14 H.-J. Lin, P. Herman, J.S. Kang, and J.R. Lakowicz, *Anal. Biochem.* **294**, 118 (2001).
- 15 A. Gafni and L. Brand, *Chem. Phys. Lett.* **58**, 346 (1978).
- 16 A. G. Ryder, S. Power, T. J. Glynn, and J. J. Morrison, *Proc SPIE – Int. Soc. Opt. Eng.* **4259**, 102 (2001).
- 17 O. S. Wolfbeis and E. Urbano, *Anal. Chem.* **55**, 1904 (1983).
- 18 P. J. Kinlen, J. E. Heider, and D. E. Hubbard. *Sens. Actuators B.* **22**, 13 (1994).
- 19 C. E. Bunker, B. Ma, K. J. Simmons, H. W. Rollins, J. T. Liu, J. J. Ma, C. W. Martin, D. D. DesMarteau, and Y. P. Sun, *J. Electroanal. Chem.* **459**, 15 (1998).
- 20 C.E. Bunker, H.W. Rollins, B. Ma., K.J. Simmons, J. T. Liu, J.J. Ma, C.W. Martin, D. D. DesMarteau, and Y. P. Sun. *J. Photochem. Photobiol. A: Chemistry*, **126**, 71 (1999).
- 21 A. Lassoued, C. Lalo, J. Deson, P. Batamack, J. Fraissard, M. A. Harmer, D. Corbin, *Chem. Phys. Lett.* **303**, 368 (1999).
- 22 P. C. Lee, and D. Meisel, *J. Am. Chem. Soc.* **102**, 5477 (1980).
- 23 A. G. Ryder, T. J. Glynn, M. Feely and A.J.G. Barwise, *Spectrochim. Acta Part A.* **58**, 1025 (2002).
- 24 R. K. Bauer, R. Borenstein, P. de Mayo, K. Okada, M. Rafalska, W.R. Ware, and K.C. Wu, *J. Am. Chem. Soc.* **104**, 4635 (1982).
- 25 J. R. Lakowicz, *Principals of Fluorescence Spectroscopy*, 2nd ed., Kluwer Academic / Plenum Publishers, New York, 1999, pp. 120 - 126.
- 26 M. Straume, S. G. Fraiser-Cadoret, and M. L. Johnson, "Least squares analysis of fluorescence data", in Topics in Fluorescence Spectroscopy, Volume 2, Principles, J.R. Lakowicz, Ed. (Plenum Press, New York, 1991), Chap. 4.
- 27 S. Power, Ph.D. Thesis National University of Ireland-Galway, 2002.
- 28 A. Lobnik, I. Oehme, I. Murlovic, and O. S. Wolfbeis, *Anal. Chim. Acta.* **367**, 159 (1998).
- 29 A. Lobnik, N. A. Majcen, K. Niederreiter, and G. Uray, *Sens. Actuators B.* **74**, 200 (2001).
- 30 M. J. P. Leiner and P. Hartmann, *Sens. Actuators B.* **11**, 281 (1993).
- 31 E. T. Ryan, T. Xiang, K. P. Johnston, and M. A. Fox, *J. Phys. Chem. A.* **101**, 1827 (1997).
- 32 L. A. Diverdi and M. R. Topp, *J. Phys. Chem.*, **88**, 3447 (1984).
- 33 C. D. Geddes, *Meas. Sci. Technol.* **12**, R53 (2001).
- 34 J. R. Lakowicz, *Principles of fluorescence spectroscopy*. (Kluwer Academic/Plenum Publishers, New York, 1999), 2nd. ed. p. 238-64; *ibid.* p. 515-30.
- 35 G. J. Mohr and O. S. Wolfbeis, *Anal. Chim. Acta.* **292**, 41 (1994).
- 36 O. S. Wolfbeis, N. V. Rodriguez, and T. Werner, *Mikrochim. Acta.* **108**, 133 (1992).
- 37 M. J. P. Leiner and O. S. Wolfbeis, "Fiber Optic pH sensors", in *Fiber Optic chemical sensors and Biosensors*. O. S. Wolfbeis ed., (CRC Press, Boca Raton, Florida 1991), Volume 1, Chapter 8.